

## Metal-Ion-Mediated Base Pairs in Nucleic Acids

Jens Müller\*<sup>[a]</sup>

**Keywords:** Bioinorganic chemistry / DNA / RNA / Nucleosides / Nucleobases

Nucleic acids and their analogues raise more and more interest in research areas outside biology and biochemistry. The functionalization of these evolutionary optimized self-assembling macromolecules with metal ions widens their applicability even further. Previous efforts to incorporate metal ions site-specifically into nucleic acids focused on the covalent attachment of appropriate ligands to either the sugar phosphate backbone or the nucleobases. More recently, the

use of metal-ion-mediated base pairs, i.e. the replacement of natural nucleobases by ligands, was suggested as an alternative means. This microreview discusses selected examples of metal-ion-mediated base pairs, including those that comprise unmodified natural nucleobases, and describes possible applications for the resulting metal-modified nucleic acids. (© Wiley-VCH Verlag GmbH & Co. KGaA, 69451 Weinheim, Germany, 2008)

### 1. Introduction

Natural deoxyribonucleic acid (DNA) is a double-helical supramolecule whose hybridization properties have been optimized by evolution over billions of years. This is one of the reasons why numerous applications far beyond its original biological relevance have evolved around this nucleic acid. Nowadays, DNA and its derivatives are being applied in such diverse areas as synthetic organic chemistry,<sup>[1]</sup> medicine,<sup>[2]</sup> biotechnology,<sup>[3,4]</sup> and materials science.<sup>[5–7]</sup> Its robustness, its predictable and programmable hybridization properties, and the high rigidity of the double helix on the nanoscale are only a few properties that make this nucleic acid an interesting candidate for various applications. Moreover, the synthesis of oligonucleotides by both chemical and biochemical methods is well established, permitting easy access to reasonable amounts of short and long DNA strands. To allow an even more extensive applicability, numerous non-natural base pairs have been implemented into DNA, thereby aiming at expanding the genetic four letter

alphabet.<sup>[8,9]</sup> These artificial base pairs can be mediated for example by hydrogen bonding,<sup>[10–12]</sup> by hydrophobic interactions,<sup>[13]</sup> or merely be based on shape complementarity.<sup>[14]</sup>

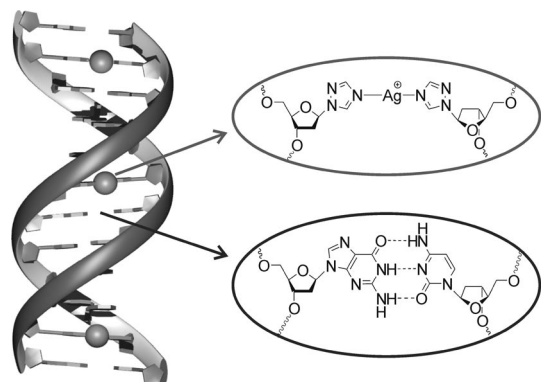
The controlled incorporation of metal ions or metal complexes into nucleic acids is a possibility to broaden the scope of their applications even further. As a result of such a site-specific addition of functional components, the metal-containing double helices are expected to display interesting chemical and physical properties. For example, it should become possible to generate nucleic acids with tailored magnetic and electric properties,<sup>[15]</sup> to store and retrieve information based on the sequence of the metal complexes or their electric or photoelectric properties,<sup>[16]</sup> or to use the chirality of the DNA double helix to induce enantioselectivity in a reaction catalyzed by the incorporated metal ion.<sup>[17]</sup> One possibility to incorporate site-specifically metal ions into a nucleic acid is the covalent attachment of suitable ligands either to the oligonucleotide backbone<sup>[16,18–35]</sup> or to the natural nucleobases.<sup>[36–40]</sup> Only recently, the use of artificial metal-ion-mediated base pairs was suggested as an alternative means.<sup>[41]</sup> In such a base pair, the natural nucleobases are replaced by ligands with a high affinity towards metal ions.<sup>[42–46]</sup> Hence, the base pair is no longer mediated by hydrogen bonds but rather by coordinative bonds to a

[a] Faculty of Chemistry, Dortmund University of Technology, Otto-Hahn-Str. 6, 44227 Dortmund, Germany  
Fax: +49 231 755 3797  
E-mail: jens.mueller@tu-dortmund.de



*Jens Müller, born in 1971, studied chemistry at Dortmund University of Technology and University College London. He received his Diploma (1996) and his PhD (1999) for work on metal-stabilized rare tautomers of nucleobases and platinum-stabilized parallel-stranded DNA, performed in the group of Professor Bernhard Lippert (Dortmund University of Technology). Supported by the Alexander von Humboldt Foundation, he spend nearly 2½ years as a postdoctoral fellow in the USA, working in the groups of Professor Stephen J. Lippard (MIT) and Professor Gerhard Wagner (Harvard Medical School) on the solution structure of the reductase component of the metallo-enzyme methane monooxygenase. In mid 2002 he returned to Dortmund University of Technology to become an Independent Research Group Leader. In 2008, he earned his Habilitation degree and became Privatdozent. His research interests comprise Bioinorganic Chemistry of Nucleic Acids, and in particular metal-ion-mediated base pairs and the characterization and utilization of nucleic acids containing these base pairs.*

central metal ion. This leads to a functionalization of the nucleic acids difficult to obtain otherwise: The metal ions can be arrayed in a geometrical fashion pre-defined by the choice of the oligonucleotide sequence. Scheme 1 shows the structural model of a DNA double helix comprising both natural and metal-ion-mediated base pairs.

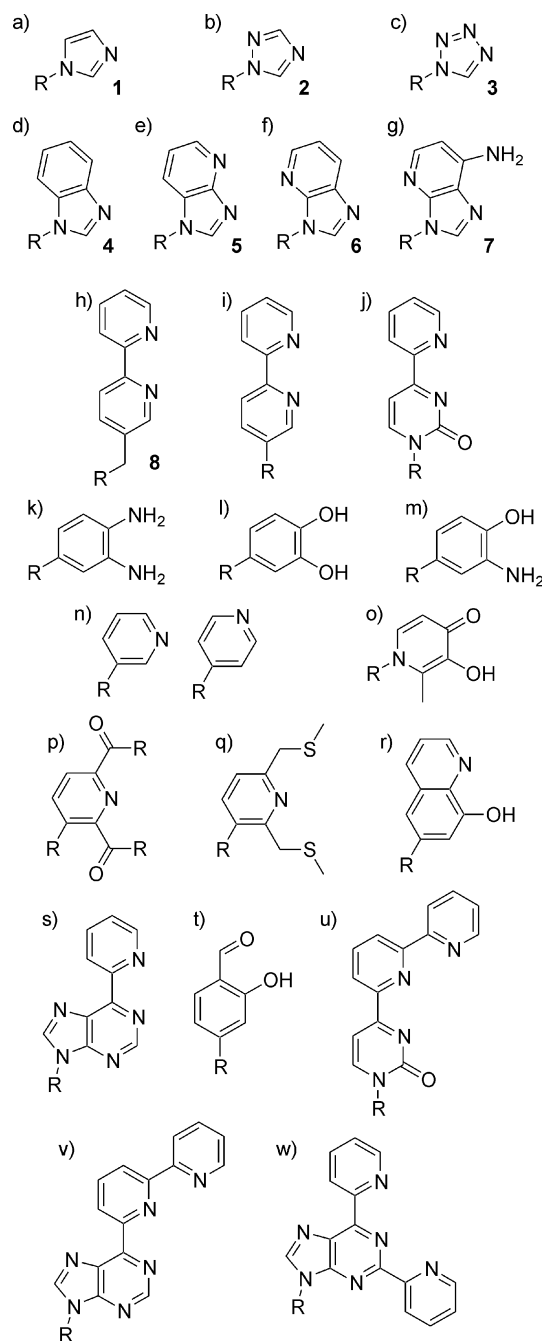


Scheme 1. Representation of a B-type DNA duplex with natural hydrogen-bond-mediated and artificial metal-ion-mediated base pairs. This figure was prepared using MOLMOL.<sup>[47]</sup>

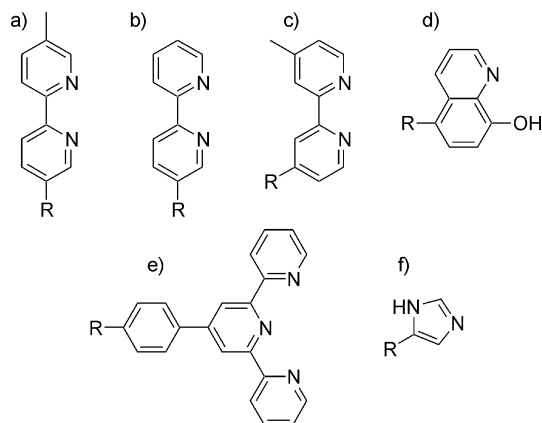
### 1.1 Metal-Ion-Mediated Base Pairs with Artificial Nucleosides

The first report on the potential use of artificial nucleosides in metal-ion-mediated base pairs was published in 1999,<sup>[41]</sup> proceeded by numerous examples in the following years. Most of these were designed for use in DNA,<sup>[48–75]</sup> but a few examples exist where metal-ion-mediated base pairs were introduced into nucleic acid analogues such as PNA (peptide nucleic acid)<sup>[76–81]</sup> or GNA (glycol nucleic acid).<sup>[65]</sup> The majority of the early publications reported on the incorporation of one or two artificial base pairs interspersed within a double helix otherwise comprising natural base pairs. More recently, the generation of oligonucleotides with three, four, five, ten, or even 19 consecutive metal-ion-mediated base pairs was reported.<sup>[50,59,60,64,70,75]</sup> Provided that orthogonal base pairs are used, even different metal ions can be incorporated site-selectively into DNA double helices.<sup>[60]</sup> Schemes 2 and 3 present an overview of artificial nucleobases that have been either suggested or actually used for the formation of metal-ion-mediated base pairs in DNA and PNA, respectively.

Up to now, the structural characterization of one double helix containing metal-ion-mediated base pairs has been reported.<sup>[62]</sup> It comprises two Cu<sup>2+</sup>-mediated base pairs of pyridine-2,6-dicarboxylate and pyridine (Scheme 2, p and n) embedded in-between natural nucleosides. The oligonucleotide sequence is derived from the palindromic Dickerson–Drew dodecamer, the archetype of B-type DNA structure,<sup>[82]</sup> by substitution of two adenine–thymine base pairs. Interestingly, the artificial nucleic acid crystallizes in the Z-DNA conformation.<sup>[62]</sup> In addition to the square planar environment provided by the artificial nucleobases, the Cu<sup>2+</sup> ion is coordinated axially by two oxygen atoms from adja-



Scheme 2. Artificial nucleosides for metal-ion-mediated base pairs in DNA (R = 2'-deoxyribose). The nucleobases are a) imidazole **1**;<sup>[49]</sup> b) 1,2,4-triazole **2**;<sup>[49,51,52]</sup> c) tetrazole **3**;<sup>[49,53]</sup> d) benzimidazole **4**;<sup>[52]</sup> e) 1*H*-imidazo[4,5-*b*]pyridine **5**;<sup>[52]</sup> f) 3*H*-imidazo[4,5-*b*]pyridine (1-deazapurine) **6**;<sup>[48,52]</sup> g) 7-amino-3*H*-imidazo[4,5-*b*]pyridine (1-deazaadenine) **7**;<sup>[50]</sup> h) 5-methyl-2,2'-bipyridine **8**;<sup>[54,66,67]</sup> i) 2,2'-bipyridine;<sup>[68]</sup> j) 4-(pyridin-2-yl)pyrimidin-2-one;<sup>[69]</sup> k) *o*-phenylenediamine;<sup>[41]</sup> l) catechol;<sup>[55]</sup> m) 2-aminophenol;<sup>[56]</sup> n) pyridine;<sup>[57,61–64,71,72]</sup> o) 3-hydroxy-2-methyl-4-pyridone;<sup>[58–60]</sup> p) R = OH: pyridine-2,6-dicarboxylic acid;<sup>[61,62]</sup> R = NH<sub>2</sub>: pyridine-2,6-dicarboxamide;<sup>[64]</sup> R = NHCH<sub>3</sub>: *N,N'*-dimethylpyridine-2,6-dicarboxamide;<sup>[64]</sup> q) 2,6-bis(methylsulfanylmethyl)pyridine;<sup>[63]</sup> r) 8-hydroxyquinoline;<sup>[65]</sup> s) 6-(pyridin-2-yl)purine;<sup>[70]</sup> t) salicylaldehyde;<sup>[60,73–75]</sup> u) 4-(2,2'-bipyridin-6-yl)pyrimidin-2-one;<sup>[71]</sup> v) 6-(2,2'-bipyridin-6-yl)purine;<sup>[72]</sup> w) 2,6-bis(pyridin-2-yl)purine.<sup>[72]</sup> Compounds **1–8** will be described in more detail in this review.



Scheme 3. Artificial nucleosides used to generate metal-ion-mediated base pairs in PNA. The artificial nucleobases are a) 5'-methyl-2,2'-bipyridine;<sup>[76]</sup> b) 2,2'-bipyridine;<sup>[78]</sup> c) 4'-methyl-2,2'-bipyridine;<sup>[80]</sup> d) 8-hydroxyquinoline;<sup>[77]</sup> e) 4'-phenyl-2,2':6',2''-terpyridine;<sup>[81]</sup> f) imidazole.<sup>[79]</sup> R indicates the point of attachment to the peptide backbone.

cent nucleosides, namely a furanose oxygen atom and a guanine keto group. The coordination of the former is only possible in the Z-type conformation. Apparently, the propensity of  $\text{Cu}^{2+}$  to adopt a distorted octahedral coordination geometry imposes this otherwise unfavourable conformation, indicating the large influence of the interspersed metal-ion-mediated base pairs on the overall DNA structure.

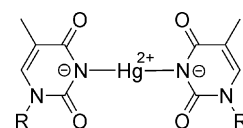
The hydroxypyridone nucleoside (Scheme 2, o) was used in the synthesis of the first series of oligonucleotides that contain consecutive rows of metal-ion-mediated base pairs.<sup>[59]</sup> A total of five self-complementary oligonucleotides  $\text{d}(\text{GH}_n\text{C})$  ( $n = 1-5$ , G = guanine, H = hydroxypyridone, C = cytosine) were synthesized, and the  $\text{Cu}^{2+}$ -binding behaviour characterized. It was shown by EPR spectroscopy that the metal ions are ferromagnetically coupled with one another to form magnetic chains. Theoretical calculations are supportive of this ferromagnetic behaviour.<sup>[83-85]</sup> From the fine-structure splitting in the EPR spectrum of the double helix formed from  $\text{d}(\text{GH}_2\text{C})$  and  $\text{Cu}^{2+}$ , an intermetallic distance of 3.7(1) was estimated, which is in the range of the distance between neighbouring base pairs in DNA. These oligonucleotides are promising candidates in the development of metal-based molecular magnets.<sup>[59]</sup>

A slightly different approach in the generation of metal-ion-mediated base pairs was taken with the salen base pair, which is formed in situ inside the double helix from two salicylaldehyde nucleosides (Scheme 2, t) located on complementary strands in the presence of excess ethylenediamine.<sup>[60,73-75]</sup> This base pair was developed against the background of a potential use of metal-modified DNA in catalysis, as the salen ligand is one of the most prominent ligands used in asymmetric catalysis.<sup>[73]</sup> The assembly of this base pair can be considered cooperative: Ethylenediamine is necessary for the formation of the ligand, and the subsequently coordinated metal ion prevents hydrolysis of

the resulting imines.<sup>[74]</sup> This cooperativity is surely one of the reasons for the enormous duplex stability associated with the metal-ion-mediated salen base pair, as can be seen from the increase in an oligonucleotide melting temperature of more than 42 °C upon establishing one  $\text{Cu}^{2+}$ -mediated salen base pair.<sup>[73]</sup> The metal complex formation is energetically so much favoured that even the disruption of a natural base pair or the distortion of the double helix is accepted.<sup>[74]</sup> The salen base pair is highly versatile in that it binds a variety of metal ions, e.g.  $\text{Cu}^{2+}$ ,  $\text{Mn}^{2+}$ ,  $\text{Ni}^{2+}$ ,  $\text{Fe}^{2+}$ , or  $\text{VO}^{2+}$ . As  $\text{Mn}^{2+}$  coordinated by a salen ligand is known to be oxidized to  $\text{Mn}^{3+}$  under aerobic conditions,<sup>[86]</sup> each resulting  $\text{Mn}^{3+}$ -mediated salen base pair carries one positive charge. Nonetheless, a DNA double helix with a continuous stack of ten identical metal-ion-mediated base pairs was generated for the first time by applying the  $\text{Mn}^{3+}$ -mediated salen base pair.<sup>[75]</sup> This is supportive of the belief that positive charge accumulated inside a DNA double helix can be compensated for by the negatively charged backbone. Indeed, DNA was shown to be able to accommodate a row of three consecutive, positively charged,  $\text{Ni}^{2+}$ -mediated artificial base pairs,<sup>[70]</sup> whereas PNA with its neutral backbone was not able to do so,<sup>[78]</sup> albeit in different sequence contexts.

## 1.2 Metal-Ion-Mediated Base Pairs with Natural Nucleosides

In addition to the use of artificial nucleosides for the formation of metal-ion-mediated base pairs, natural nucleosides can be applied as well. It is known from early studies on the interaction of nucleic acids with  $\text{Hg}^{2+}$  that this metal ion is preferentially coordinated by thymine residues.<sup>[87-90]</sup> Later, model studies showed that upon substitution of the thymine imide proton, linear thymine- $\text{Hg}^{2+}$ -thymine (T-Hg-T) complexes are formed (Scheme 4).<sup>[91]</sup> More recently it was shown that this structural motif can be inserted systematically into DNA double helices.<sup>[92-98]</sup> The applicability of DNA containing T-Hg-T base pairs in terms of a molecular wire was investigated by using theoretical approaches. These showed that the metal ion does not participate in mediating long-distance radical cation hopping in DNA,<sup>[99,100]</sup> but that it might play an important role in excess electron transfer.<sup>[99]</sup>



Scheme 4.  $\text{Hg}^{2+}$ -mediated base pair (T-Hg-T) comprising two deprotonated thymine residues (R, R' = 2'-deoxyribose).

A few years ago, a rearrangement of regular B-DNA to so-called M-DNA was reported to occur at elevated pH values in the presence of divalent metal ions such as  $\text{Zn}^{2+}$ ,  $\text{Co}^{2+}$ , or  $\text{Ni}^{2+}$ .<sup>[101,102]</sup> As this rearrangement is accompanied by an acidification of the solution, substitution of some of the nucleobase protons involved in hydrogen bonds by the

metal ions was suggested to take place, namely one proton per metal ion. This should lead to metal-ion-mediated base pairs similar to the T–Hg–T one.<sup>[102]</sup> M-DNA was reported to possess metal-like conductivity,<sup>[103]</sup> contrary to the behaviour of the underlying B-DNA. The proposed long-range electron transfer<sup>[104–106]</sup> would enable self-assembling DNA-based nanoelectronic devices, and a recent theoretical investigation suggests the formation of a field-effect transistor from M-DNA.<sup>[107]</sup> However, the precise structures of the metal-ion-mediated base pairs in M-DNA,<sup>[108,109]</sup> the enhanced conductivity of M-DNA,<sup>[110–112]</sup> and even its actual formation are controversially discussed.<sup>[113]</sup> Moreover, single-crystal X-ray diffraction analyses of DNA oligonucleotides crystallized under alkaline conditions in the presence of Zn<sup>2+</sup>, Co<sup>2+</sup>, or Ni<sup>2+</sup> do not show incorporation of the metal ions inside the double helix but rather a coordination via the N7 positions of terminal guanine residues.<sup>[114]</sup> Nonetheless, the bottom-up approach of using *artificial* metal-ion-mediated base pairs with their known geometry is a promising path towards DNA-based devices with a precisely controllable composition.

### 1.3 Artificial Nucleosides Described in this Review

The expected broad applicability of metal-modified nucleic acids led to a quest for new artificial nucleosides that are compatible with the formation of metal-ion-mediated base pairs. In this review, a summary of our work on eight non-natural nucleosides (compounds **1–8** in Scheme 2) is described with respect to the characterization of their metal-ion-binding behaviour, their incorporation into oligonucleotides, and/or their use in metal-ion-mediated base pairs. In addition, the application of the natural nucleoside uridine (U) in connection with the formation of U–Hg–U base pairs in RNA double helices is discussed. Throughout this paper, experimentally characterized compounds are denoted by Arabic numerals, molecules investigated by density functional theory (DFT) methods by Roman numerals, and oligonucleotides by OL- followed by an Arabic numeral.

## 2. Characterization of the Artificial Nucleosides

Before the formation of any potential metal-ion-mediated base pair within an oligonucleotide double helix, the reactivity of the artificial nucleoside(s) towards the respective metal ion should be investigated thoroughly. For example, monodentate ligands might be able to support not only double but also triple helix formation.<sup>[57]</sup> In addition, it is worthwhile to establish the acid-base properties of the nucleoside, i.e. whether the protonation of the nucleoside must be expected to compete with the metalation or not.

### 2.1 Acidity Constants

The  $pK_a$  values of various protonated artificial nucleosides were determined. Table 1 gives an overview of the acidity constants. Because in most cases the  $\alpha$  anomer of

the respective nucleoside had been obtained as a side product,  $pK_a$  values are listed for this anomer, too. Obviously, for the nucleosides under consideration no competition between protonation and metalation reaction is to be expected when working in the physiological pH range, because all acidity constants are well below the value of seven. Furthermore, depending on the number of endocyclic nitrogen atoms in the azole nucleobase and the presence or absence of aromatic rings appended to it, a broad range of  $pK_a$  values from about –3 to 6.42(5) is covered by these artificial nucleosides. As the affinity towards a metal ion typically shows the same trend as the affinity towards a proton, this would translate into a graded stability of the metal-ion-mediated base pairs, a feature that might be interesting in applications of the metal-modified nucleic acids.

Table 1.  $pK_a$  values of protonated artificial 2'-deoxyribonucleosides.<sup>[48,49,52]</sup>

Nucleoside	$\alpha$ anomer <sup>[a]</sup>	$\beta$ anomer <sup>[a]</sup>	$\Delta pK_a$ ( $\alpha - \beta$ ) <sup>[a]</sup>
Imidazole <b>1</b>	6.42(5)	6.01(5)	0.41(7)
1,2,4-Triazole <b>2</b>	1.53(5)	1.32(5)	0.21(7)
Tetrazole <b>3</b>	< –3 <sup>[b]</sup>	< –3 <sup>[b]</sup>	
Benzimidazole <b>4</b>	4.45(3)	4.21(3)	0.24(4)
1 <i>H</i> -Imidazo[4,5- <i>b</i> ]pyridine <b>5</b>	3.45(2)	3.26(2)	0.19(3)
3 <i>H</i> -Imidazo[4,5- <i>b</i> ]pyridine <b>6</b>	3.15(2)	2.84(2)	0.31(3)

[a] The errors given correspond to three times the standard deviations of the mean values ( $3\sigma$ ). [b] Estimate based on the  $pK_a$  value of 1-methyltetrazole ( $pK_a = -3$ ).<sup>[115]</sup>

One interesting feature of the artificial nucleosides covered by Table 1 regards the inherently different  $pK_a$  values of the  $\alpha$  and  $\beta$  anomers. Obviously, protonated 2'-deoxy- $\beta$ -D-ribonucleosides are slightly more acidic than the corresponding 2'-deoxy- $\alpha$ -D-ribonucleosides, with  $\Delta pK_a$  values ranging from 0.19(3) to 0.41(7). To confirm independently the differential reactivity of the anomers towards protonation and to investigate the underlying reasons, density functional theory (DFT) calculations at the B3LYP/6-311+G\*\* level were performed using 1,2,4-triazole nucleoside **2** as an example.<sup>[52]</sup> The result of these calculations is in very good agreement with the experimental data [ $\Delta pK_a = 0.16$  vs. 0.21(7)]. Interestingly, no significant differences in the charge distribution between sugar moiety and nucleobase were observed between the two anomers, ruling out different charge localizations as a reason for the different acidity. Instead, the distinct values for  $\Delta pK_a$  can be attributed to a differential influence of the protonation on the extent of the anomeric effect. An increased interaction of the oxygen lone pair of the sugar moiety with the antibonding orbital of the glycosidic bond due to a more favourable overlap is typically considered the reason for the anomeric effect.<sup>[116]</sup> Upon protonation of nucleoside **2**, the increase in this interaction is indeed more pronounced for the  $\alpha$  anomer, resulting in a larger stabilization of the protonated  $\alpha$  nucleoside and concomitantly in a more acidic protonated  $\beta$  nucleoside. Unfortunately, no sufficiently precise data are available on the  $pK_a$  values of the  $\alpha$  anomeric counterparts of the natural 2'-deoxy- $\beta$ -D-ribonucleosides. Published values could be interpreted in a way that an identical trend



in reactivity also exists for the natural nucleosides [e.g. 2'-deoxyguanosine:  $pK_a(\alpha \text{ anomer}) = 2.6$ ,  $pK_a(\beta \text{ anomer}) = 2.3$ ]<sup>[117]</sup> but the relatively large standard deviations of those values do not permit a reliable, final conclusion to be drawn.

## 2.2 Stoichiometry and Stability Constants

To allow the formation of metal-ion-mediated base pairs, the monodentate azole-based artificial nucleosides need to form stable complexes with linearly coordinating metal ions in a 2:1 ratio. In this respect,  $Ag^+$  and  $Hg^{2+}$  were chosen because they are known to adopt a linear coordination geometry but at the same time are flexible enough to accommodate more than two ligands as might become necessary during the formation of a potential triple helix. The stoichiometries of selected complexes of metal ions and artificial nucleosides were determined by applying the method of continuous variations, i.e. by preparing Job plots,<sup>[49]</sup> prior to incorporating the respective nucleosides into oligonucleotides. The overview of the results (Table 2) shows that only a few metal ion complexes of imidazole- or triazole-based nucleosides are able to adopt the 2:1 stoichiometry that is necessary for base pair formation. In no case, 3:1 complexes reminiscent of a base triple were observed. As was shown by using triazole nucleoside as an example, no differences exist for the  $\alpha$  and the  $\beta$  anomer, respectively.

Table 2. Stoichiometries of selected complexes of azole nucleosides.<sup>[49,52]</sup>

Nucleoside	Complex with $Ag^+$	Complex with $Hg^{2+}$
Imidazole <b>1<math>\beta</math></b>	2:1	2:1
1,2,4-Triazole <b>2<math>\alpha</math></b>	2:1	1:1
1,2,4-Triazole <b>2<math>\beta</math></b>	2:1	1:1
Tetrazole <b>3<math>\beta</math></b>	1:1	no complex formation

Whereas the relative stabilities of the metal ion complexes can be estimated by comparing different Job plots – with sharp maxima implying a high stability – the determination of the exact stability constants requires additional experiments. Therefore, the nucleosides were titrated with increasing amounts of metal ion solutions, and the chemical shifts of their aromatic protons were followed by  $^1H$  NMR spectroscopy.<sup>[49,52]</sup> Individual formation constants were calculated from the experimental data by using the computer program EQNMR.<sup>[118]</sup> Table 3 provides a list of these stability constants.

Several conclusions can be drawn from the data presented in Table 3. First, the complex  $[Ag(2\beta)_2]^+$  apparently does not obey the generic rule that the second individual stability constant is smaller than the first one. Although such behaviour is known for other complexes of triazole derivatives<sup>[120]</sup> as well as for other  $Ag^+$  complexes such as  $[Ag(NH_3)_2]^+$ , it might in this case be the result of poor data convergence in the determination of  $\log \beta_1$  caused by almost identical chemical shifts for the complexes  $[Ag(2\beta)]^+$  and  $[Ag(2\beta)_2]^+$ . Second, **2 $\alpha$**  forms more stable complexes than **2 $\beta$** , a finding that was confirmed independently by DFT

Table 3. Overall stability constants (water) for metal ion complexation of selected artificial azole-based nucleosides.<sup>[49,52]</sup>

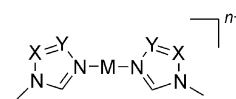
Nucleoside	$Ag^+$		$Hg^{2+}$	
	$\log \beta_1$ <sup>[a]</sup>	$\log \beta_2$ <sup>[a]</sup>	$\log \beta_1$ <sup>[a]</sup>	$\log \beta_2$ <sup>[a]</sup>
Imidazole <b>1<math>\beta</math></b>	> 5 <sup>[b]</sup>	> 10 <sup>[b]</sup>	> 5 <sup>[b]</sup>	> 10 <sup>[b]</sup>
1,2,4-Triazole <b>2<math>\alpha</math></b>	n.d. <sup>[c]</sup>	4.9(2)	2.07(6)	–
1,2,4-Triazole <b>2<math>\beta</math></b>	1.5(7)	4.3(1)	1.56(4)	–
Tetrazole <b>3<math>\beta</math></b>	0.86(2)	–	–	–

[a] The errors given correspond to three times the standard deviations of the mean values ( $3\sigma$ ) or the possible systematic error, whichever is larger. [b] Estimate based on the occurrence of an abrupt change of slope in the binding curves of **1 $\beta$**  with  $Ag^+$  or  $Hg^{2+}$ .<sup>[119]</sup> [c] not determined.

methods<sup>[52]</sup> and that goes along well with the observation that **2 $\beta$**  is less basic (see section 2.1). Third, all listed complexes are more stable than Watson–Crick base pairs in water. Contrary to the complexes reported here, the formation of regular Watson–Crick pairs cannot be observed in water due to their significant destabilization by the solvent.<sup>[121]</sup> Hence, in terms of stability, metal-ion-mediated base pairs from azole nucleosides should be able to replace regular Watson–Crick base pairs within DNA double helices.

## 2.3 Structural Studies of Model Complexes

To obtain structural insights into the geometry of the metal-ion-mediated base pairs, studies have been performed applying either DFT calculations or X-ray diffraction of suitable single crystals of model complexes. Regarding the putative metal-ion-mediated base pairs that include two azole nucleosides and  $Ag^+$  or  $Hg^{2+}$ , DFT calculations were performed with 1-methylazoles as nucleoside analogues (Scheme 5). After geometry optimization, the energy difference  $\Delta E$  with respect to a fully planar structure with *cisoid* methyl groups as necessary for a Watson–Crick base pair surrogate was determined.<sup>[49]</sup> All energy differences lie between 0.8 and 4.0 kJ mol<sup>−1</sup> and are therefore small enough to allow a reasonably high population of the planar conformation as required for a proper implementation into an oligonucleotide double helix. Furthermore, the loss in energy due to formation of a coplanar complex is expected to be more than compensated for by stacking interactions between neighbouring base pairs. The C(methyl)–C(methyl) distances  $d$  of the planar complexes represent the distances between glycosidic bonds in the DNA duplex. Especially the values of those azole/metal combinations that favour the formation of 2:1 complexes  $\{[Ag(1\beta)_2]^+$ ,  $[Ag(2\beta)_2]^+$ , and  $[Hg(1\beta)_2]^{2+}$ ; see Table 2} resemble the average distance between glycosidic bonds in idealized B-DNA.<sup>[49]</sup> Therefore,



Scheme 5. Structures used in the DFT calculations ( $M = Ag^+$ ,  $n = 1$  or  $M = Hg^{2+}$ ,  $n = 2$ ; **I**:  $X, Y = CH$ ; **II**:  $X = N, Y = CH$ ; **III**:  $X, Y = N$ ).<sup>[49]</sup>

imidazole nucleoside **1** or 1,2,4-triazole nucleoside **2** together with  $\text{Ag}^+$  or  $\text{Hg}^{2+}$  are promising building blocks for metal-ion-mediated base pairs.

1-Deazapurine can formally be viewed as an imidazole moiety with an appended pyridine ring. Hence, 1-deazapurine nucleoside **6** can be considered a derivative of imidazole nucleoside **1** with modified properties such as increased size and decreased basicity (see Table 1). In an attempt to model a putative homo base pair of 1-deazapurine nucleoside **6** mediated by a  $\text{Hg}^{2+}$  ion, the corresponding methyl derivative 9-methyl-1-deazapurine (9-MeDP) was synthesized and reacted with  $\text{Hg}(\text{CF}_3\text{COO})_2$ . In the presence of  $\text{NaNO}_3$ , colourless crystals of  $[\text{Hg}(9\text{-MeDP})_2](\text{NO}_3)_2 \cdot \text{H}_2\text{O}$  **9** were obtained that were suitable for a structure determination.<sup>[48]</sup> As required for a metal-ion-mediated base pair, the nucleobase surrogates are arranged approximately *trans* to each other [ $173.1(1)^\circ$ ]. However, the deazapurine planes are oriented at an angle of  $82.98(7)^\circ$ . The methyl groups are in a *transoid* orientation which is incompatible with regular Watson–Crick base pairing. Nonetheless, against the background of the relatively small energy differences between optimized and planar *cisoid* geometry as calculated for the metal-ion-mediated base pairs with azole nucleosides, it can be anticipated that incorporation of **6** into oligonucleotides might still lead to the formation of double helices with metal-ion-mediated base pairs.

In addition to generating homo base pairs from azole nucleosides, the latter may also be applied in the formation of hetero base pairs with tridentate complementary nucleosides, e.g. based on terpyridine. To study whether such systems are feasible or not, model complexes of the artificial nucleobases were prepared from  $[\text{M}(\text{terpy})(\text{H}_2\text{O})]^{2+}$ , using metal ions that are well-known for adopting the required square-planar geometry ( $\text{M} = \text{Pd}^{\text{II}}, \text{Pt}^{\text{II}}$ ).<sup>[53]</sup> Potential sites of attachment of the sugar residue to the terpyridine nucleobase are either the  $\text{C4}'$  carbon (see Figure 1) of terpyridine or the methyl group of 4'-methyl-2,2':6',2''-terpyridine (see Figure 2). Reaction with 1-methylimidazole, acting as a surrogate for imidazole nucleoside **1**, led to the formation of  $[\text{M}(\text{terpy})(1\text{-methylimidazole})](\text{ClO}_4)_2$  (**10**:  $\text{M} = \text{Pd}^{\text{II}}$ ; **11**:  $\text{M} = \text{Pt}^{\text{II}}$ ). In these complexes, the dihedral angle between the square-planar coordination sphere of the metal ion and the imidazole ring amounts to  $73.9(3)^\circ$  (**10**) and  $74.0(2)^\circ$  (**11**). Analyses of the respective  $^1\text{H}$  NMR spectra suggest that the solution structures closely resemble those found in the solid state. Apparently, a steric clash between the terpyridine  $\text{H6}/\text{H6}''$  protons and the imidazole  $\text{H2}/\text{H4}$  protons (Figure 1, a) prohibits the formation of a planar complex. However, it might be possible to drive the system to planarity, e.g. by the energy gained from  $\pi$  stacking interactions with neighbouring base pairs in an oligonucleotide.

Replacement of the 1-methylimidazole ligand in **11** by 1-methyltetrazole, acting as a surrogate for tetrazole nucleoside **3**, should lead to a planar structure because the formal substitution of two C–H groups by nitrogen atoms reduces the steric clashes and should result in the formation of C–H...N hydrogen bonds instead. However, in 1-methyltetrazole three different nitrogen atoms are available for coordina-

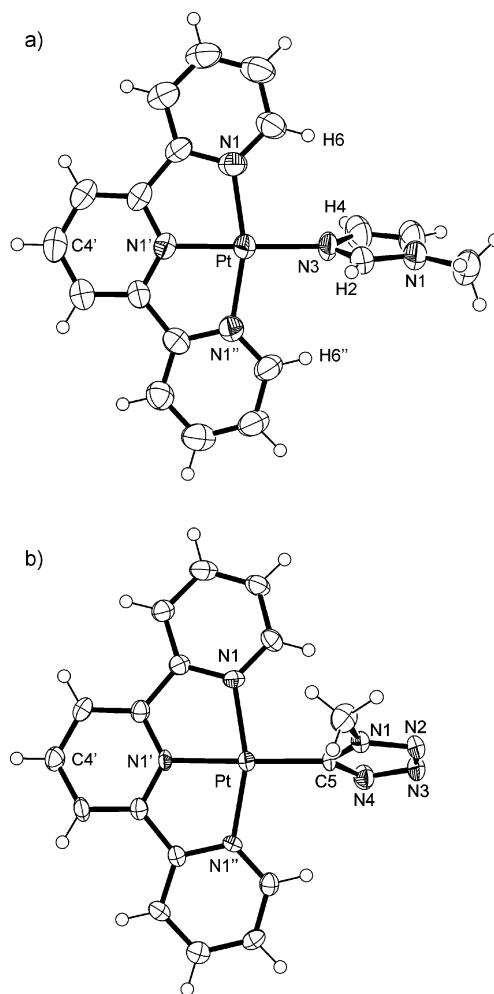


Figure 1. View of the cations of a) compound **11** and b) compound **12**. Selected atoms are labelled according to the numbering schemes of the respective individual ligands. The sugar moiety of the prospective nucleoside could be attached via  $\text{C4}'$ . Figure adapted from ref.<sup>[53]</sup>

tion, and only metal binding to  $\text{N3}$  is expected to give rise to a planar complex. To much of our surprise, the complex formed upon reaction of  $[\text{Pt}(\text{terpy})(\text{H}_2\text{O})]^{2+}$  with 1-methyltetrazole comprises a deprotonated 1-methyltetrazolate coordinated via its carbon atom  $\text{C5}$  (Figure 1, b).<sup>[53]</sup> Although such a coordination pattern is not unprecedented, the product  $[\text{Pt}(\text{terpy})(1\text{-methyltetrazolate})]\text{ClO}_4$  **12** is the first structurally characterized complex of this type that was synthesized directly from its ligands. The tetrazolate moiety in **12** is oriented at an angle of  $67.0(2)^\circ$  with respect to the platinum coordination sphere.  $^1\text{H}$  NMR studies confirm the presence of the organometallic entity in solution, too. Attempts to obtain the desired planar complex by using different reaction conditions led to the isolation of the doubly metalated compound  $[\{\text{Pt}(\text{terpy})\}_2(1\text{-methyltetrazolate})](\text{ClO}_4)_3$  **13**, in which the  $\text{Pt}(\text{terpy})^{2+}$  moieties are attached to  $\text{N4}$  and  $\text{C5}$ . An analogous palladium(II) complex  $[\{\text{Pd}(\text{terpy})\}_2(1\text{-methyltetrazolate})](\text{ClO}_4)_3$  **14** was obtained likewise.<sup>[53]</sup> While the exact mechanism for the formation of the organometallic species is still unknown, it is tempting

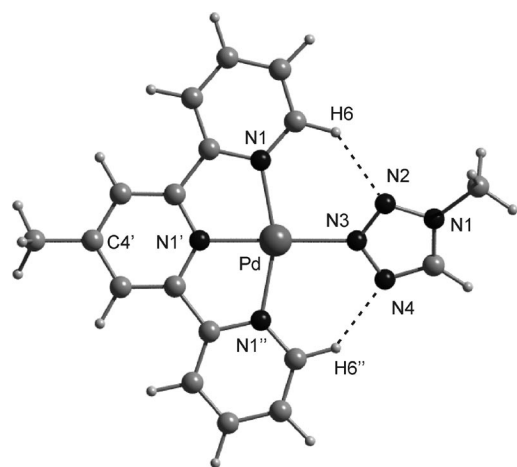


Figure 2. View of the geometry-optimized structure of  $[\text{Pd}(4'\text{-methyl-2,2':6',2''-terpyridine})(1\text{-methyltetrazole-}N3)]^{2+}$  as calculated by DFT methods. Intramolecular hydrogen bonds are depicted as dashed lines. Selected atoms are labelled according to the numbering schemes of the respective individual ligands. The sugar moiety of the prospective nucleoside could be attached via the methyl group at  $C4'$ . Figure adapted from ref.<sup>[53]</sup>

to speculate that a concerted substitution mechanism with essentially simultaneous C–H deprotonation and carbon metalation takes place.<sup>[53]</sup> A feasible scenario for the second metalation step is that complex **12** is an intermediate in the formation of **13**, and that the second  $\text{Pt}(\text{terpy})^{2+}$  entity is guided to the  $N4$  atom by an initial attraction via  $\pi$  stacking interactions with the carbon-bonded first  $\text{Pt}(\text{terpy})^{2+}$  group.

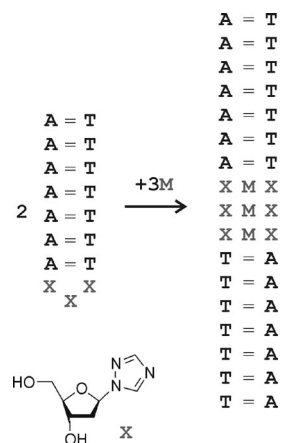
To obtain a geometric model for the putative planar metal-ion-mediated base pair from terpyridine, tetrazole, and  $\text{Pd}^{2+}$ , DFT calculations were performed (Figure 2).<sup>[53]</sup> In concurrent calculations, the tetrazole ligand was replaced by other monodentate ligands such as imidazole, 1,2,4-triazole, and pyridine for reasons of better comparison. Only the complex comprising tetrazole adopts a conformation in which the two ligands are *not* oriented perpendicularly. Furthermore, the energy necessary to convert the structure from the optimized to a fully planar geometry amounts to only  $0.8 \text{ kJ mol}^{-1}$ , as compared to  $70\text{--}151 \text{ kJ mol}^{-1}$  in the other cases where steric hindrance prohibits a planar geometry. The angle between the square-planar coordination sphere of  $\text{Pd}^{2+}$  and the tetrazole plane amounts to only  $27.9^\circ$  for the fully optimized geometry. As expected, the planarization is driven by the formation of two hydrogen bonds from the aromatic terpyridine protons  $H6$  and  $H6''$  to the tetrazole nitrogen atoms  $N2$  and  $N4$ , respectively (Figure 2).

These model studies show that the formation of metal-ion-mediated base pairs from terpyridine and a monodentate ligand should be possible. Ideally, tetrazole nucleoside **3** should serve as the latter ligand because the resulting base pair could adopt a planar geometry provided that tetrazole is coordinating to the metal ion via its  $N3$  atom. The applicability of artificial nucleosides related to the other monodentate ligands under investigation, i.e. imidazole nucleoside **1**, 1,2,4-triazole nucleoside **2**, and pyridine

nucleoside, cannot be ruled out completely. Despite unfavourable geometries of the model complexes, the potential base pairs might experience additional stabilization within the nucleic acid. Indeed, the incorporation of related base pairs from terpyridine-like ligands, pyridine, and  $\text{Ag}^+$  into a short oligonucleotide double helix was reported recently (Scheme 2, u–w and n).<sup>[71,72]</sup>

### 3. Metal-Ion-Induced Conformational Change in Artificial Oligonucleotides

Because 1,2,4-triazole nucleoside **2** was shown to be able to differentiate between  $\text{Ag}^+$  and  $\text{Hg}^{2+}$  via formation of complexes with different stoichiometries, this nucleoside was selected for incorporation into a nucleic acid. Sequence  $d(\text{A}_7\text{X}_3\text{T}_7)$  **OL-1** ( $\text{A}$  = adenine,  $\text{T}$  = thymine,  $\text{X}$  = 1,2,4-triazole) comprises stretches of both natural and artificial nucleosides arranged in a way that a hairpin structure can be adopted in which the artificial nucleosides are located in the loop (Scheme 6). In the presence of an appropriate metal ion, two oligonucleotide strands could also form a regular double helix with metal-ion-mediated base pairs. Due to the lacking capability of triazole nucleoside to engage in hydrogen bonds, formation of such a duplex is not expected in the absence of transition metal ions, as it would contain destabilizing mispairs.



Scheme 6. Conformational change of oligonucleotide **OL-1** from hairpin to regular double helix, accompanied by the formation of metal-ion-mediated base pairs ( $\text{A}$  = adenine,  $\text{T}$  = thymine,  $\text{X}$  = triazole,  $\text{M} = \text{Ag}^+$ ).<sup>[51]</sup>

The formation of a regular double helix prior to the addition of transition metal ions was also ruled out experimentally based on two observations.<sup>[51]</sup> First, the melting temperature  $T_m$  of **OL-1** is concentration-independent. Second, by applying a labelling scheme in which fluorescence is quenched due to Förster resonance energy transfer (FRET) in the presence of a regular double helix yet remains unchanged in the presence of a hairpin structure, formation of the latter could be unequivocally confirmed.

Not unexpectedly, addition of  $\text{Hg}^{2+}$  to a solution of **OL-1** led to a decrease in  $T_m$  of approximately  $2^\circ\text{C}$  per equivalent of added  $\text{Hg}^{2+}$ .<sup>[51]</sup> In this context, one equivalent of



metal ions corresponds to one metal ion per potential metal-ion-mediated base pair in a regular duplex, i.e. for 1 nmol of d(A<sub>7</sub>X<sub>3</sub>T<sub>7</sub>) **OL-1**, one equivalent of Hg<sup>2+</sup> translates into 1.5 nmol of Hg<sup>2+</sup>. The destabilizing effect of Hg<sup>2+</sup> might be due to its preference to form 1:1 adducts with triazole nucleoside **2** (see section 2.2). Furthermore, because of the high affinity of thymine towards Hg<sup>2+</sup>, the undesired formation of such adducts might also be responsible for the destabilization. Contrary to Hg<sup>2+</sup>, the addition of Ag<sup>+</sup> had a large stabilizing effect on **OL-1**. Interestingly, the melting temperatures of the resulting adduct were found to be dependent on the oligonucleotide concentration, suggesting that **OL-1** no longer adopts a hairpin conformation in the presence of Ag<sup>+</sup>.<sup>[51]</sup> UV spectroscopy was used to gain insight into the concomitant conformational change. From these measurements it became clear that the first equivalent of Ag<sup>+</sup> interacts differently with the oligonucleotide than excess Ag<sup>+</sup>, which was conveniently explained by the preferential formation of metal-ion-mediated base pairs prior to additional, non-specific interactions of excess Ag<sup>+</sup>.<sup>[51]</sup>

Mass spectrometry is a method typically used to indicate the presence of metal-ion-mediated base pairs within a modified nucleic acid. In the case of **OL-1**, MALDI-TOF mass spectrometry was applied.<sup>[51]</sup> Unfortunately, the mass spectra indicated that most of the duplex dissociates under the experimental conditions. However, the spectra did contain peaks that could be assigned to the double helix and its Ag<sup>+</sup> adducts. A comparison with the spectra of identical samples in the absence of Ag<sup>+</sup> was clearly indicative of an Ag<sup>+</sup>-induced stabilization of the regular duplex, which in turn is supportive of the formation of metal-ion-mediated base pairs.

Dynamic light scattering (DLS) was used to determine the size of the oligonucleotide in solution.<sup>[51]</sup> Accordingly, a solution of **OL-1** contains 100 mass percent of particles with a mean hydrodynamic radius  $r_H$  of 1.6(1) nm prior to the addition of Ag<sup>+</sup> (Table 4). In the presence of one equivalent of Ag<sup>+</sup>,  $r_H$  increases to 2.10(5) nm, a typical value for a duplex with 17 base pairs. The increase of  $r_H$  of approximately 30% that accompanies the structural transition was also observed in a related system of RNA with Hg<sup>2+</sup>-mediated base pairs (see section 6).

Table 4. Hydrodynamic radii of **OL-1** and reference oligonucleotides.<sup>[51]</sup>

Oligonucleotide	$r_H^{[a]}$ / nm	Mass / %	Polydispersity <sup>[b]</sup> / %
<b>OL-1</b>	1.6(1)	100	7.3
<b>OL-1</b> + Ag <sup>+</sup>	2.10(5)	99.9	7.4
reference hairpin <b>OL-2</b> <sup>[c]</sup>	1.55(5)	99.9	8.4
reference duplex <b>OL-3</b> <sup>[d]</sup>	2.05(5)	99.9	7.0

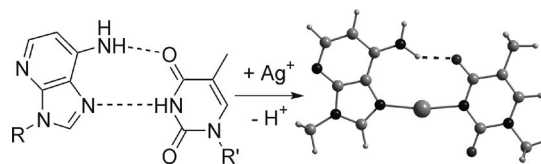
[a] The hydrodynamic radii correspond to the average values from at least four measurements. [b] A polydispersity of <15% indicates that the sample is monomodal monodispers. [c] **OL-2**: d(A<sub>7</sub>GAAT<sub>7</sub>). [d] **OL-3**: d(GGAAAAGGAGAGAAGAA)·(TTCTTCTCTCCTTTTCC).

In conclusion, the appropriate design of an oligonucleotide sequence enables the synthesis of an artificial nucleic acid whose structure can be modified by the addition of

suitable metal ions. Such a system might be developed into a modularly built metal-ion sensor by appending fluorescence markers and quenchers to the nucleic acids. Depending on the choice of the artificial nucleoside, different metal-ion selectivities can be expected for this type of sensor.

#### 4. Base Pairs Mediated by Hydrogen Bonding and Metal-Ion-Binding

When natural hydrogen-bond-mediated base pairs are formally substituted by metal-ion-mediated ones, the thermal stability of the resulting nucleic acid typically increases due to the higher stability of coordinative bonds compared to hydrogen bonds. While this stabilization is often considered a positive effect of the incorporation of metal-ion-mediated base pairs, it might turn into a disadvantage once longer continuous stacks of artificial base pairs are prepared. As a result of the increased stability, the DNA strands might lose their ability to self-assemble reversibly.<sup>[122]</sup> It was therefore highly desirable to devise an artificial base pair that has a thermal stability comparable to that of a natural base pair yet is mediated by a metal ion. Towards this end, 1-deazaadenine (D) and thymine (T) were chosen as complementary nucleobases.<sup>[50]</sup> Earlier reports had suggested that the oligonucleotides d(D<sub>20</sub>) and d(T<sub>20</sub>) associate via the Hoogsteen edge of the purine base to form a double helix.<sup>[123,124]</sup> Scheme 7 shows how a metal-ion-mediated base pair is derived from such a Hoogsteen pair by the substitution of a proton by a metal ion. As was shown by DFT methods, the resulting metal-ion-mediated base pair can be expected to comprise one remaining hydrogen bond.<sup>[50]</sup>



Scheme 7. Proposed formation of a base pair from 1-deazaadenine and thymine, mediated by an Ag<sup>+</sup> ion and a hydrogen bond. Shown on the right is the geometry-optimized structure modelled by DFT calculations.<sup>[50]</sup>

Two oligonucleotides comprising 1-deazaadenine nucleoside **7** were synthesized and characterized, namely d(ADA-DADADA)·d(T<sub>9</sub>) **OL-4** and d(D<sub>19</sub>A)·d(T<sub>20</sub>) **OL-5**.<sup>[50]</sup> In both cases, the addition of Ag<sup>+</sup> ions led to a significant increase in  $T_m$ , with a maximum value of  $T_m$  reached in the presence of one equivalent of Ag<sup>+</sup>. Obviously, the maximum stability is reached at a stoichiometric ratio of one Ag<sup>+</sup> ion per base pair.<sup>[50]</sup> For example, the melting temperature of **OL-5** was found to increase from about 10 °C in the absence of transition metal ions to 51.2 °C in the presence of one equivalent of Ag<sup>+</sup>. Additionally, a series of UV spectra of **OL-5** with increasing amounts of Ag<sup>+</sup> displayed changes only during the addition of the first equivalent of metal ion, with excess Ag<sup>+</sup> not influencing the spectrum



any further (Figure 3).<sup>[50]</sup> The CD spectra of **OL-5** prior to and after addition of  $\text{Ag}^+$  were found to be almost identical, with only minor variations being observed, namely a bathochromic shift of about 3 nm of the minima at 213 and 256 nm as well as of the maximum at 226 nm.<sup>[50]</sup> As CD spectra are sensitive to alterations of the helical structure, the lack of major differences was taken as an indication that only subtle structural changes take place upon addition of  $\text{Ag}^+$ . This is exactly what is expected when substituting a proton by an  $\text{Ag}^+$  ion.

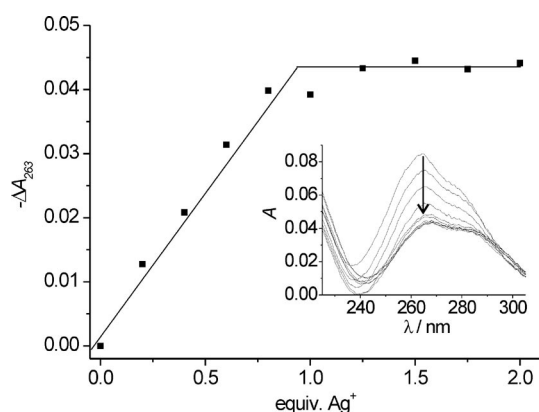


Figure 3. UV absorption changes at 263 nm upon addition of  $\text{AgNO}_3$  to **OL-5**. Inset: UV spectra of **OL-5** in the presence of various amounts of  $\text{AgNO}_3$ . The arrow indicates the direction of the changes. Figure adapted from ref.<sup>[50]</sup>

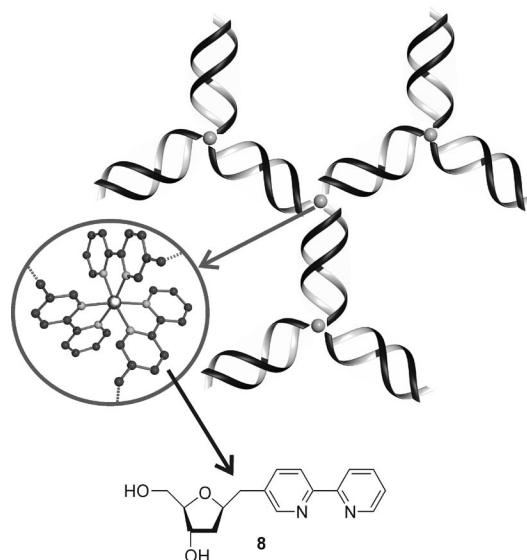
Hence, the base pair formed from 1-deazaadenine and thymine in the presence of  $\text{Ag}^+$  was the first example of a new class of artificial base pairs mediated by hydrogen bonding and metal-ion-binding. The increment in  $T_m$  of approximately 2 °C per base pair corresponds nicely to the values of 2 °C and 3 °C, respectively, that are typically assumed when estimating the contributions of adenine-thymine and guanine-cytosine base pairs to the melting temperature of oligonucleotides under physiological conditions. Hence, its stability is comparable to that of natural base pairs, yet it is mediated by a metal ion. It therefore combines the reliable self-assembly of hydrogen-bonded base pairs with the properties of metal-ion-mediated ones. The two examples reported so far show that the novel base pair can be used in different sequence contexts, and that even the generation of a long continuous stretch of metal-ion-mediated base pairs can be accomplished, making it a valuable addition to the repertoire of structural elements in DNA nanotechnology.

## 5. Metal-Ion-Induced Aggregation of Bipyridine-Containing Oligonucleotides

Metal-ion-mediated base pairs need to adopt a (more or less) planar geometry so that they can be incorporated into a duplex without loss of stabilizing  $\pi$  stacking interactions between adjacent base pairs. However, artificial ligand-based nucleosides may be used in combination with metal ions that prefer non-planar coordination geometries in a

different context, i.e. in the generation of DNA-based nanostructures. In the past decade, more and more examples of the application of nucleic acids in the creation of well-defined two- and three-dimensional nanostructures have been reported. These include, amongst others, a cube,<sup>[125]</sup> a smiley face,<sup>[126]</sup> and autonomously shape-shifting structures.<sup>[127]</sup> Most recently, even the use of DNA as a mediator in the crystallization of gold nanoparticles was convincingly demonstrated.<sup>[128,129]</sup> The employment of non-Watson–Crick base pairs is expected to extend the scope of this type of nanoarchitecture. Along these lines, ligands attached directly or via short linkers to oligonucleotides can be used to control the assembly of nucleic acids.<sup>[16,18–30,33]</sup> Besides this application, the use of ligand-modified DNA oligonucleotides for the sequence-specific detection of nucleic acids has also been reported.<sup>[31,34,35,37]</sup> However, the use of a ligand-based nucleoside in the generation of higher-order DNA structure was only reported by us recently.<sup>[54]</sup>

A reasonable approach to using ligand-based nucleosides for the assembly of higher-order DNA structures is their incorporation at the end of an oligonucleotide. After double helix formation, these nucleosides represent single-stranded overhangs that can become sticky ends in the presence of appropriate metal ions. For example, nucleoside **8** was incorporated at the 5'-end of the otherwise self-complementary DNA sequence d(BCGCGAATTCGCG) **OL-6** (B = nucleoside **8**). It was envisaged that the addition of  $\text{Fe}^{2+}$  would lead to the formation of octahedral complexes  $[\text{Fe}(\mathbf{8})_3]^{2+}$ , which in turn would result in the assembly of nanoscale DNA-based networks (Scheme 8).<sup>[54]</sup>



Scheme 8. Representation of a DNA-based network connected via metal-ion coordination of nucleoside **8** attached terminally to oligonucleotide double helices. Figure adapted from ref.<sup>[54]</sup> Coordinates of the structure shown in the inset derived from ref.<sup>[130]</sup>

Atomic force microscopy (AFM) images of **OL-6** in the absence of transition metal ions, using mica as surface support, showed a homogeneous surface without any indication for the presence of DNA. This is in agreement with

expectations, because individual double helices of **OL-6** – estimated to be about 4 nm long – cannot be visualized due to the limited lateral resolution of AFM. However, AFM images obtained in the presence of  $\text{Fe}^{2+}$  displayed an entirely different topology (Figure 4), indicative of the aggregation of DNA in the form of higher-order structures.<sup>[54]</sup> Two distinct types of structures were observed: The first one, shown also in the lower panel of Figure 4, consists of monolayers of DNA duplexes. Its morphology is reminiscent of that reported for bipyridine-modified quadruple helices in the presence of  $\text{Co}^{2+}$  or  $\text{Zn}^{2+}$ .<sup>[24]</sup> The second type of structure is a disc-shaped one with a height of up to 60 nm. It must therefore either be composed of several layers of DNA or comprise a complex three-dimensional network of double helices. The top panel of Figure 4 shows one occurrence of the monolayer structure and five examples of a disc. Unexpectedly, within a few hours after sample preparation, the disc-shaped aggregates evolved into fewer fibre-like structures with lengths of several nanometres while maintaining their height of up to 60 nm.<sup>[54]</sup> Storage under dry argon stalled the morphological change: The evolution from disc-shaped to fibre-like structures apparently started upon introduction of the sample into the microscope, i.e. upon its exposure to air. The reasons for this structural evolution are not known yet; it appears as if the humidity of the surrounding gas plays an important role.

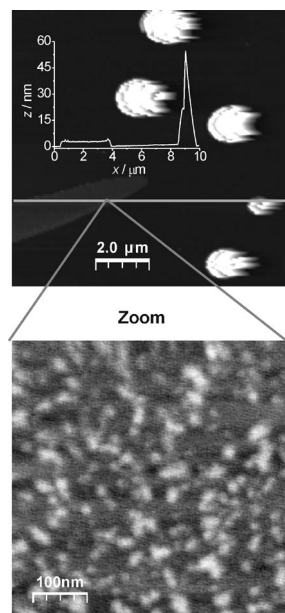


Figure 4. AFM topography images of d(BCGCGAATTCGCG) **OL-6** (**B** = 2,2'-bipyridine-based nucleoside **8**) on mica in the presence of  $\text{Fe}^{2+}$ . The inset in the top image shows the associated height profile. Figure adapted from ref.<sup>[54]</sup>

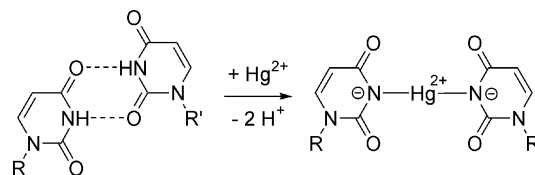
In summary, these experiments showed that palindromic DNA oligonucleotides terminally appended with the artificial 2,2'-bipyridine-based nucleoside **8** form higher-order structures in the presence of  $\text{Fe}^{2+}$ . The aggregation can be explained by the formation of  $[\text{Fe}(\mathbf{8})_3]^{2+}$  complexes, thereby creating cross-links between neighbouring duplexes. Such systems can be regarded as artificial three-way junctions

that assemble only in the presence of appropriate metal ions and represent a first step towards an application of ligand-based nucleosides in the assembly of defined DNA nanostructures.

## 6. RNA with Mercury(II)-Mediated Base Pairs

While several examples exist of metal-ion-mediated base pairs in DNA<sup>[48–75]</sup> or PNA,<sup>[76–81]</sup> their systematic incorporation into RNA had not been reported until recently.<sup>[131]</sup> Prior to our study on  $\text{Hg}^{2+}$ -mediated base pairs in RNA,<sup>[131]</sup> only one example had been published in which an  $\text{Au}^{3+}$ -mediated guanine-cytosine pair was coincidentally formed in RNA crystals with about 40% occupancy while soaking those crystals in a solution of  $\text{AuCl}_3$ .<sup>[132]</sup> The lack of systematic studies might have been in part due to the fact that RNA is often considered a complex, three-dimensional structure with only a few double helical regions. Furthermore, the ribose in RNA is certainly more prone to hydrolytic decomposition than the 2'-deoxyribose in DNA. On the other hand, the formation of regular RNA double helices is only dependent on an optimal sequence design. Moreover, RNA duplexes are significantly more stable against hydrolysis than single strands, because in the former the 2'-OH group is not in the correct geometrical position for a nucleophilic attack of the adjacent phosphodiester bridge.<sup>[133,134]</sup> Therefore, RNA double helices must not be discarded as scaffolds for the arrangement of metal ions. On the contrary, as a result of the different conformations of RNA and DNA duplexes, distinct relative orientations of the metal ions and therefore distinct physical and chemical properties can be expected.

Experiments regarding the incorporation of metal-ion-mediated base pairs into RNA double helices were performed with uracil (U) as the designated metalated nucleobase. Its DNA counterpart thymine is well-known for forming T–Hg–T base pairs,<sup>[91–98]</sup> hence an analogous behaviour was expected for uracil. Scheme 9 shows how the  $\text{Hg}^{2+}$ -mediated base pair U–Hg–U could form from a *cis*-UU wobble pair.



Scheme 9. Proposed formation of a  $\text{Hg}^{2+}$ -mediated base pair (U–Hg–U) from a *cis*-UU wobble pair ( $\text{R}, \text{R}'$  = ribose of an RNA backbone).<sup>[131]</sup>

### 6.1 General Synthesis and Characterization of RNA

Five different RNA constructs **OL-7** to **OL-11** (Table 5) were synthesized by in vitro transcription with T7 RNA polymerase.<sup>[131]</sup> Whereas duplexes **OL-7** and **OL-8** are non-palindromic, **OL-9** to **OL-11** are self-complementary and

may form either a hairpin or a regular double helix. The number of consecutive uracil residues varies between two and twenty, allowing the investigation of both the capability of T7 polymerase to insert long stretches of identical nucleotides and a potential upper limit of consecutive metal-ion-mediated base pairs. The syntheses showed that up to six consecutive identical nucleotides do not pose a problem for T7 polymerase. When lining up more nucleotides of the same kind, the polymerase loses its fidelity by one nucleotide position.<sup>[131]</sup>

Table 5. Sequences of RNA constructs **OL-7** to **OL-11**.<sup>[131]</sup>

Sequence	U–Hg–U <sup>[a]</sup>
<b>OL-7</b> 5'–r (GGAGCGCGU <sub>2</sub> GUCCCUC)–3'	2
3'–r (CCUCGCGCU <sub>2</sub> CAGGGAG)–5'	
<b>OL-8</b> 5'–r (GGAGCGCGU <sub>6</sub> GUCCCUC)–3'	6
3'–r (CCUCGCGCU <sub>6</sub> CAGGGAG)–5'	
<b>OL-9</b> 5'–r (GGAGCGCGU <sub>6</sub> CGCGCUCC)–3'	6
<b>OL-10</b> 5'–r (GGAGU <sub>10</sub> CUCC)–3'	10
<b>OL-11</b> 5'–r (GGAGU <sub>20</sub> CUCC)–3'	20

[a] Maximum number of potential U–Hg–U base pairs.

For all RNA oligonucleotides under consideration, the addition of one equivalent of Hg<sup>2+</sup> was accompanied by increasing melting temperatures  $T_m$ .<sup>[131]</sup> Going along with the number of central uracil residues, the increase in  $T_m$  varied from 1 °C (**OL-7**) via 18 °C (**OL-8**) and 23 °C (**OL-10**) to 50 °C (**OL-11**).<sup>[131]</sup> This clear trend suggests that the stabilization occurs via formation of U–Hg–U base pairs. In the case of **OL-9**, a comparison of the  $T_m$  before and after the addition of Hg<sup>2+</sup> is not meaningful because of the different conformations adopted under these conditions (see below).

DLS and DOSY (diffusion-ordered spectroscopy) were applied as independent methods to measure the hydrodynamic radii  $r_H$  of the RNA constructs (Table 6).<sup>[131]</sup> To discriminate between hairpin and double helix, their respective theoretical hydrodynamic radii were calculated, too. In the absence of Hg<sup>2+</sup>, the good agreement of calculated and measured  $r_H$  suggests that **OL-7** and **OL-8** adopt duplex structures, whereas **OL-9** forms a hairpin. The constructs with ten or more consecutive uracil residues, i.e. **OL-10** and **OL-11**, appear to adopt multiple conformations as deduced from the diverging experimental values of  $r_H$ , probably as a result of their long non-Watson–Crick regions.

In the presence of Hg<sup>2+</sup>, the hydrodynamic radii of duplexes **OL-7** and **OL-8** remain (more or less) constant. This is in agreement with the imide protons of oppositely located uracil residues being replaced by Hg<sup>2+</sup> (Scheme 9), because such a substitution should proceed without an overall change of the helix size. On the contrary, the hydrodynamic radius of **OL-9** shows an approximate 30%-increase upon addition of Hg<sup>2+</sup>, indicative of double helix formation. Apparently, the duplex structure is now more stable than the hairpin, as conveniently explained by the formation of U–Hg–U base pairs. The 30%-increase in size is in agreement with the observations made for the conformational change of the triazole-containing oligonucleotide **OL-1** (see section 3). Earlier work on T–Hg–T base pairs in DNA had shown

Table 6. Hydrodynamic radii  $r_H$  of **OL-7** to **OL-11** as determined by DLS ( $r_{H,DLS}$ ) and DOSY ( $r_{H,DOSY}$ ) before and after addition of 1.2 equiv. of Hg<sup>2+</sup>. Shown is also the theoretical hydrodynamic radius  $r_H$ . If the sequence is able to form either hairpin or duplex, theoretical values are given for both conformations.<sup>[131]</sup>

	Hairpin	Duplex	Without Hg <sup>2+</sup>		With Hg <sup>2+</sup>	
	$r_H$	$r_H$	$r_{H,DOSY}^{[a]}$	$r_{H,DLS}^{[a]}$	$r_{H,DOSY}^{[a]}$	$r_{H,DLS}^{[a]}$
<b>OL-7</b>	–	2.21	2.1(1)	2.13(2)	2.2(3)	2.23(2)
<b>OL-8</b>	–	2.00	2.3(1)	2.00(2)	2.4(2)	1.69(2)
<b>OL-9</b>	1.43	2.04	1.6(1)	1.56(2)	2.1(2)	2.26(5)
<b>OL-10</b>	1.17	2.34	1.5(4)	1.74(4)	2.2(4)	2.08(5)
<b>OL-11</b>	1.82	2.28	1.8(1)	2.40(5)	2.8(9)	2.65(6) <sup>[b]</sup>

[a] All values are average values of at least five measurements. [b] This sample showed a high polydispersity in the DLS measurements.

that hairpins comprising loops of two or three thymine residues can rearrange to double helices with two or three metal-ion-mediated base pairs. Contrary to this, a hairpin with a loop of four thymine residues does not rearrange but forms a metal cross-link between the first and the fourth thymine.<sup>[92]</sup> Our results obtained with **OL-9** show that hairpins with larger loops are again able to form duplexes with metal-ion-mediated base pairs. Presumably, intrastrand cross-links within a hairpin loop can only be formed if the nucleosides are prearranged in a geometrically correct fashion. The structural changes that occur upon addition of Hg<sup>2+</sup> to **OL-10** and **OL-11** could not be derived conclusively. In both cases, the clear increase in  $r_H$  could be indicative of double helix formation, but the high polydispersity observed especially for **OL-11** suggests that again a complex mixture of different duplexes is formed. Prolonged treatment of metal-modified **OL-7** to **OL-11** with the chelating resin Chelex was shown to remove Hg<sup>2+</sup> from the U–Hg–U base pairs.<sup>[131]</sup> Interestingly, Chelex had been reported *not* to remove Hg<sup>2+</sup> from T–Hg–T base pairs in DNA.<sup>[96]</sup> Presumably, the wider A-form RNA helix allows a facilitated attack compared to B-DNA. Alternatively, the thymine nucleobases might bind more strongly to the metal ion than the uracil nucleobases do.

## 6.2 Detailed Study of Oligonucleotide **OL-9**

Due to the conformational change that accompanies the addition of Hg<sup>2+</sup> to **OL-9**, this oligonucleotide had been subjected to a more detailed study. The <sup>1</sup>H, <sup>1</sup>H NOESY spectrum of **OL-9** in the absence of Hg<sup>2+</sup> was clearly indicative of a well-structured loop formed by the six central uridine residues.<sup>[131]</sup> Characteristic cross-peaks verified the presence of the A-form helix in the stem region. By using <sup>15</sup>N and <sup>13</sup>C-labeled **OL-9**, the nitrogen resonances of all seven uracil residues in **OL-9** could be unambiguously assigned. After the addition of Hg<sup>2+</sup>, only the resonances of the N3 nitrogen atoms of the six central uracil residues were completely broadened out, whereas all N1 resonances and the N3 resonance of the uracil residue from the adenine–uracil base pair remained detectable.<sup>[131]</sup> Moreover, the H6–C6 cross-peaks in a <sup>1</sup>J<sub>HC</sub>–HSQC spectrum of five of the six



central uracil residues shifted strongly in the presence of  $\text{Hg}^{2+}$ , whereas the other two were more or less unaffected.<sup>[131]</sup> Taken together, these NMR spectroscopic data are strongly supportive of the formation of U–Hg–U base pairs.

The structural changes upon addition of  $\text{Hg}^{2+}$  to **OL-9** were also monitored by CD spectroscopy.<sup>[131]</sup> In the absence of transition metal ions, the CD spectrum of **OL-9** resembles that of typical A-form RNA (Figure 5).<sup>[135,136]</sup> Stepwise addition of  $\text{Hg}^{2+}$  leads to a diminishment of the minimum and the maximum, and the maximum experiences a red shift of about 8 nm. Two isosbestic points indicate that during the addition of the first equivalent of  $\text{Hg}^{2+}$ , the A-form shape of the helix is not disrupted. Excess  $\text{Hg}^{2+}$  binds differently, which can be seen from the fact that the isosbestic points are no longer observed. Considering that all four nucleotides are potential binding sites for metal ions,<sup>[137]</sup> such differential binding is not unexpected. It appears as if the first equivalent of  $\text{Hg}^{2+}$  is incorporated into U–Hg–U base pairs, whereas additional  $\text{Hg}^{2+}$  binds in a random fashion to other coordination sites available in the nucleic acid.

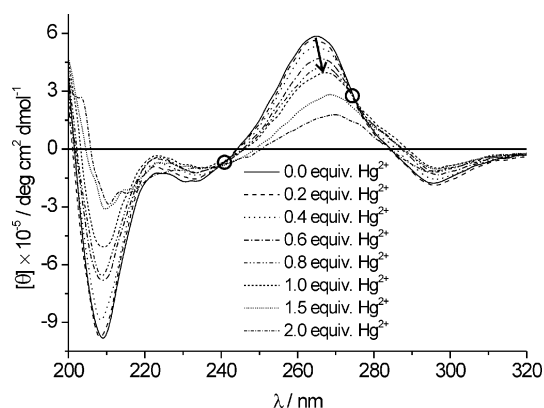


Figure 5. CD spectra of **OL-9** upon addition of  $\text{Hg}^{2+}$ . Arrows indicate the directions of the changes. Two isosbestic points are observed at 240 nm and 275 nm (black circles) during the addition of the first equiv. of  $\text{Hg}^{2+}$ . Figure adapted from ref.<sup>[131]</sup>



Figure 6. A-form model of the duplex formed from **OL-9** in the presence of  $\text{Hg}^{2+}$ . This Figure was prepared using MOLMOL.<sup>[47]</sup>

In summary, T7 RNA polymerase, used to synthesize the oligonucleotides **OL-7** to **OL-11** by in vitro transcription, is able to insert long stretches of identical nucleobases. Probably unexpected by many, RNA is capable of forming duplexes with metal-ion-mediated base pairs. The resulting metal-modified nucleic acids are stable for at least a couple of months. Due to the A-form shape of the helices, the metal ions in U–Hg–U base pairs are twisted around the helical axis (Figure 6), leading to a geometrical arrangement distinct from that of metal ions in analogously modified B-type DNA and hence to different chemical and physical properties of the metal-modified nucleic acid.

## 7. Conclusions and Outlook

The introduction of imidazole, 1,2,4-triazole and tetrazole nucleosides **1–3** as nucleosides for metal-ion-mediated base pairs led to the first comprehensive study on an entire family of artificial nucleosides, namely the azole nucleosides.<sup>[49]</sup> While imidazole nucleoside **1** and 1,2,4-triazole nucleoside **2** are capable of forming metal-ion-mediated homo base pairs, tetrazole nucleoside **3** appears to be a good candidate for metal-ion-mediated hetero base pairs with a tridentate ligand as the complementary nucleobase. With its large number of endocyclic nitrogen atoms, an almost planar structure of terpyridine and N3-coordinating tetrazole should be feasible, additionally stabilized by two C–H...N hydrogen bonds.<sup>[53]</sup> In the future, such a base pair – predicted to be stable by DFT calculations – will need to be characterized experimentally, too.

The incorporation of 1,2,4-triazole nucleosides into the loop of a hairpin-forming oligonucleotide leads to a system that changes its conformation to a regular duplex in the presence of appropriate metal ions.<sup>[51]</sup> This concept of modifying the nucleic acid conformation by adding suitable metal ions provides the opportunity to design a modular metal-ion sensor. In this sensor, the metal ion affinity can be tuned by choosing an appropriate artificial nucleoside. Labelling the oligonucleotides with fluorescence donor and quencher groups should therefore enable the generation of fluorescent turn-on sensors.<sup>[51]</sup>

The  $\text{Ag}^+$ -mediated base pair from 1-deazaadenine and thymine is the first example of an artificial metal-ion-mediated base pair with a thermal stability comparable to that of its regular Watson–Crick counterparts.<sup>[50]</sup> This feature makes it highly interesting, as it allows the reversible self-assembly of metal-modified DNA containing several artificial base pairs. By using this base pair, an oligonucleotide was synthesized that contains the longest stack of consecutive metal-ion-mediated base pairs reported so far, namely 19.<sup>[50]</sup> Such continuous stacks are important for the investigation of the electronic properties of metal-modified DNA.

In the same respect, the first report on a systematic incorporation of metal-ion-mediated base pairs into RNA represents another important step forward.<sup>[131]</sup> Here, access to continuous stacks of metal ions is gained by incorporating U–Hg–U base pairs into double-stranded RNA synthe-



sized by in vitro transcription. Although initial experiments showed that the transcription fidelity of T7 RNA polymerase decreases when ten or more consecutive identical nucleotides are incorporated, it is quite possible that an optimization of the transcription conditions or a mutation of the enzyme enhances its capability to synthesize these special nucleic acids. This challenge will certainly have to be addressed in the near future, possibly also in combination with the more general question to what extent artificial nucleotides can be handled by polymerases.<sup>[138]</sup>

Addition of a ligand-based nucleoside to the end of an otherwise self-complementary oligonucleotide enables the formation of higher-order structures in the presence of appropriate metal ions.<sup>[54]</sup> Although the resulting complexes cannot necessarily be considered metal-ion-mediated base pairs, they still represent interesting building blocks that might have an impact on DNA-based nanoarchitecture. In an extension of the concept first introduced by Seeman,<sup>[139]</sup> the combination of ligand-containing nucleosides and metal ions enables a systematic formation of stable connections between individual double helices. Furthermore, the metal-ion-mediated three-way junctions that assemble from 2,2'-bipyridine-modified oligonucleotides in the presence of octahedrally coordinating metal ions might become useful as connections for DNA-based nanowires once these are applied in the formation of electric nanocircuits.<sup>[54]</sup>

Now that numerous reports on different types of artificial metal-ion-mediated base pairs have appeared since their introduction in 1999, the time has come to intensify efforts to investigate the applicability of metal-modified DNA.<sup>[122]</sup> The work summarized in this article shall help to lay the foundation for several potential applications, e.g. as metal ion sensors, as molecular wires, or as building blocks in DNA-based nanotechnology. Various additional applications are also conceivable, including the use in catalysis,<sup>[17]</sup> and maybe even in medicinal chemistry.<sup>[140]</sup> Obviously, the necessity for an expansion of the current repertory of artificial nucleosides still remains. Such an extension could be done by developing additional sulfur-containing nucleosides to be able to coordinate also softer metal ions, or by creating pairs of orthogonal metal-ion-mediated base pairs. Furthermore, the development of new approaches towards the generation of even longer continuous stacks of metal ions is of great importance for possible applications of these metal-modified nucleic acids. Nonetheless, it is probably not exaggerating to state that we are now at the onset of transferring our knowledge of how to generate metal-ion-mediated base pairs to investigating and exploiting the properties of the resulting metal-modified nucleic acids.

## Acknowledgments

I thank Dr. Fabian-Alexander Polonius, Dr. Dominik Böhme, Nicole Düpre, and Dominik A. Megger as well as my international collaboration partners Prof. Roland K. O. Sigel, Dr. Félix Zamora, and Dr. Eva Freisinger, all of whom were involved in the research described in this review. Financial support of our work by the Deutsche Forschungsgemeinschaft (DFG) within the frame of the

Emmy Noether Programme (MU1750/1-1, MU1750/1-2, and MU1750/1-3) and the ERA Chemistry network (MU1750/2-1) as well as by the Faculty of Chemistry of the Dortmund University of Technology, by the Fond der Chemischen Industrie, and by COST D39 is gratefully acknowledged.

- [1] X. Li, D. R. Liu, *Angew. Chem. Int. Ed.* **2004**, *43*, 4848–4870.
- [2] C. Potera, *Nat. Biotechnol.* **2007**, *25*, 497–499.
- [3] C. M. Niemeyer, C. A. Mirkin, *Nanobiotechnology*, Wiley-VCH, Weinheim, **2004**.
- [4] Y. Lu, J. Liu, *Curr. Opin. Biotechnol.* **2006**, *17*, 580–588.
- [5] C. M. Niemeyer, *Angew. Chem. Int. Ed.* **2001**, *40*, 4128–4158.
- [6] U. Feldkamp, C. M. Niemeyer, *Angew. Chem. Int. Ed.* **2006**, *45*, 1856–1876.
- [7] N. C. Seeman, *Nature* **2003**, *421*, 427–431.
- [8] E. T. Kool, *Acc. Chem. Res.* **2002**, *35*, 936–943.
- [9] I. Hirao, *Curr. Opin. Chem. Biol.* **2006**, *10*, 622–627.
- [10] S. A. Benner, *Acc. Chem. Res.* **2004**, *37*, 784–797.
- [11] S. R. Lynch, H. Liu, J. Gao, E. T. Kool, *J. Am. Chem. Soc.* **2006**, *128*, 14704–14711.
- [12] A. H. F. Lee, E. T. Kool, *J. Am. Chem. Soc.* **2005**, *127*, 3332–3338.
- [13] A. K. Ogawa, Y. Wu, D. L. McMinn, J. Liu, P. G. Schultz, F. E. Romesberg, *J. Am. Chem. Soc.* **2000**, *122*, 3274–3287.
- [14] E. T. Kool, H. O. Sintim, *Chem. Commun.* **2006**, 3665–3675.
- [15] T. Carell, C. Behrens, J. Gierlich, *Org. Biomol. Chem.* **2003**, *1*, 2221–2228.
- [16] K. M. Stewart, L. W. McLaughlin, *J. Am. Chem. Soc.* **2004**, *126*, 2050–2057.
- [17] G. Roelfes, *Mol. Biosyst.* **2007**, *3*, 126–135.
- [18] L. Zapata, K. Bathany, J.-M. Schmitter, S. Moreau, *Eur. J. Org. Chem.* **2003**, 1022–1028.
- [19] J. S. Choi, C. W. Kang, K. Jung, J. W. Yang, Y. G. Kim, H. Han, *J. Am. Chem. Soc.* **2004**, *126*, 8606–8607.
- [20] K. M. Stewart, L. W. McLaughlin, *Chem. Commun.* **2003**, 2934–2935.
- [21] K. M. Stewart, J. Rojo, L. W. McLaughlin, *Angew. Chem. Int. Ed.* **2004**, *43*, 5808–5811.
- [22] E. C. Constable, V. Chaurin, C. E. Housecroft, A. Wirth, *Chimia* **2005**, *59*, 832–835.
- [23] G. Bianké, V. Chaurin, M. Egorov, J. Lebreton, E. C. Constable, C. E. Housecroft, R. Häner, *Bioconjug. Chem.* **2006**, *17*, 1441–1446.
- [24] D. Miyoshi, H. Karimata, Z.-M. Wang, K. Koumoto, N. Sugimoto, *J. Am. Chem. Soc.* **2007**, *129*, 5919–5925.
- [25] J. L. Czapinski, T. L. Sheppard, *J. Am. Chem. Soc.* **2001**, *123*, 8618–8619.
- [26] J. L. Czapinski, T. L. Sheppard, *Bioconjug. Chem.* **2005**, *16*, 169–177.
- [27] K. V. Gothelf, R. S. Brown, *Chem. Eur. J.* **2005**, *11*, 1062–1069.
- [28] I. Vargas-Baca, D. Mitra, H. J. Zullyniak, J. Banerjee, H. F. Sleiman, *Angew. Chem. Int. Ed.* **2001**, *40*, 4629–4632.
- [29] D. Mitra, N. Di Cesare, H. F. Sleiman, *Angew. Chem. Int. Ed.* **2004**, *43*, 5804–5808.
- [30] H. Yang, H. F. Sleiman, *Angew. Chem. Int. Ed.* **2008**, *47*, 2443–2446.
- [31] J. Brunner, R. Kraemer, *J. Am. Chem. Soc.* **2004**, *126*, 13626–13627.
- [32] A. Mokhir, A. Kiel, D.-P. Hertel, R. Kraemer, *Inorg. Chem.* **2005**, *44*, 5661–5666.
- [33] M. Göritz, R. Krämer, *J. Am. Chem. Soc.* **2006**, *127*, 18016–18017.
- [34] N. Graf, R. Krämer, *Chem. Commun.* **2006**, 4375–4376.
- [35] N. Graf, M. Göritz, R. Krämer, *Angew. Chem. Int. Ed.* **2006**, *45*, 4013–4015.
- [36] D. J. Hurley, Y. Tor, *J. Am. Chem. Soc.* **1998**, *120*, 2194–2195.
- [37] H. S. Joshi, Y. Tor, *Chem. Commun.* **2001**, 549–550.

- [38] B. Algueró, J. López de la Osa, C. González, E. Pedroso, V. Marchán, A. Grandas, *Angew. Chem. Int. Ed.* **2006**, *45*, 8194–8197.
- [39] B. Algueró, E. Pedroso, V. Marchán, A. Grandas, *J. Biol. Inorg. Chem.* **2007**, *12*, 901–911.
- [40] K. Tanaka, K. Tainaka, T. Umemoto, A. Nomura, A. Okamoto, *J. Am. Chem. Soc.* **2007**, *129*, 14511–14517.
- [41] K. Tanaka, M. Shionoya, *J. Org. Chem.* **1999**, *64*, 5002–5003.
- [42] M. Shionoya, K. Tanaka, *Curr. Opin. Chem. Biol.* **2004**, *8*, 592–597.
- [43] K. Tanaka, M. Shionoya, *Chem. Lett.* **2006**, *35*, 694–699.
- [44] K. Tanaka, M. Shionoya, *Coord. Chem. Rev.* **2007**, *251*, 2732–2742.
- [45] G. H. Clever, C. Kaul, T. Carell, *Angew. Chem. Int. Ed.* **2007**, *46*, 6226–6236.
- [46] W. He, R. M. Franzini, C. Achim, *Prog. Inorg. Chem.* **2007**, *55*, 545–611.
- [47] R. Koradi, M. Billeter, K. Wüthrich, *J. Mol. Graphics* **1996**, *14*, 51–55.
- [48] J. Müller, F.-A. Polonius, M. Roitzsch, *Inorg. Chim. Acta* **2005**, *358*, 1225–1230.
- [49] J. Müller, D. Böhme, P. Lax, M. Morell Cerdà, M. Roitzsch, *Chem. Eur. J.* **2005**, *11*, 6246–6253.
- [50] F.-A. Polonius, J. Müller, *Angew. Chem. Int. Ed.* **2007**, *46*, 5602–5604.
- [51] D. Böhme, N. Düpre, D. A. Megger, J. Müller, *Inorg. Chem.* **2007**, *46*, 10114–10119.
- [52] J. Müller, D. Böhme, N. Düpre, M. Mehring, F.-A. Polonius, *J. Inorg. Biochem.* **2007**, *101*, 470–476.
- [53] J. Müller, E. Freisinger, P. Lax, D. A. Megger, F.-A. Polonius, *Inorg. Chim. Acta* **2007**, *360*, 255–263.
- [54] N. Düpre, L. Welte, J. Gómez-Herrero, F. Zamora, J. Müller, *Inorg. Chim. Acta* **2008**, *361*, in press (doi: 10.1016/j.ica.2007.12.005).
- [55] H. Cao, K. Tanaka, M. Shionoya, *Chem. Pharm. Bull.* **2000**, *48*, 1745–1748.
- [56] K. Tanaka, M. Tasaka, H. Cao, M. Shionoya, *Eur. J. Pharm. Sci.* **2001**, *13*, 77–83.
- [57] K. Tanaka, Y. Yamada, M. Shionoya, *J. Am. Chem. Soc.* **2002**, *124*, 8802–8803.
- [58] K. Tanaka, A. Tengeiji, T. Kato, N. Toyama, M. Shiro, M. Shionoya, *J. Am. Chem. Soc.* **2002**, *124*, 12494–12498.
- [59] K. Tanaka, A. Tengeiji, T. Kato, N. Toyama, M. Shionoya, *Science* **2003**, *299*, 1212–1213.
- [60] K. Tanaka, G. H. Clever, Y. Takezawa, Y. Yamada, C. Kaul, M. Shionoya, T. Carell, *Nature Nanotech.* **2006**, *1*, 190–194.
- [61] E. Meggers, P. L. Holland, W. B. Tolman, F. E. Romesberg, P. G. Schultz, *J. Am. Chem. Soc.* **2000**, *122*, 10714–10715.
- [62] S. Atwell, E. Meggers, G. Spraggon, P. G. Schultz, *J. Am. Chem. Soc.* **2001**, *123*, 12364–12367.
- [63] N. Zimmermann, E. Meggers, P. G. Schultz, *J. Am. Chem. Soc.* **2002**, *124*, 13684–13685.
- [64] N. Zimmermann, E. Meggers, P. G. Schultz, *Bioorg. Chem.* **2004**, *32*, 13–25.
- [65] L. Zhang, E. Meggers, *J. Am. Chem. Soc.* **2005**, *127*, 74–75.
- [66] H. Weizman, Y. Tor, *Chem. Commun.* **2001**, 453–454.
- [67] H. Weizman, Y. Tor, *J. Am. Chem. Soc.* **2001**, *123*, 3375–3376.
- [68] C. Brotschi, C. J. Leumann, *Nucleosides Nucleotides Nucleic Acids* **2003**, *22*, 1195–1197.
- [69] C. Switzer, D. Shin, *Chem. Commun.* **2005**, 1342–1344.
- [70] C. Switzer, S. Sinha, P. H. Kim, B. D. Heuberger, *Angew. Chem. Int. Ed.* **2005**, *44*, 1529–1532.
- [71] D. Shin, C. Switzer, *Chem. Commun.* **2007**, 4401–4403.
- [72] B. D. Heuberger, D. Shin, C. Switzer, *Org. Lett.* **2008**, *10*, 1091–1094.
- [73] G. H. Clever, K. Polborn, T. Carell, *Angew. Chem. Int. Ed.* **2005**, *44*, 7204–7208.
- [74] G. H. Clever, Y. Söhl, H. Burks, W. Spahl, T. Carell, *Chem. Eur. J.* **2006**, *12*, 8708–8718.
- [75] G. H. Clever, T. Carell, *Angew. Chem. Int. Ed.* **2007**, *46*, 250–253.
- [76] D.-L. Popescu, T. J. Parolin, C. Achim, *J. Am. Chem. Soc.* **2003**, *125*, 6354–6355.
- [77] R. M. Watson, Y. A. Skorik, G. K. Patra, C. Achim, *J. Am. Chem. Soc.* **2005**, *127*, 14628–14639.
- [78] R. M. Franzini, R. M. Watson, G. K. Patra, R. M. Breece, D. L. Tierney, M. P. Hendrich, C. Achim, *Inorg. Chem.* **2006**, *45*, 9798–9811.
- [79] A. Küsel, J. Zhang, M. Alvarino Gil, A. C. Stückl, W. Meyer-Klaucke, F. Meyer, U. Diedrichsen, *Eur. J. Inorg. Chem.* **2005**, 4317–4324.
- [80] B. P. Gilmartin, K. Ohr, R. L. McLaughlin, R. Koerner, M. E. Williams, *J. Am. Chem. Soc.* **2005**, *127*, 9546–9555.
- [81] K. Ohr, R. L. McLaughlin, M. E. Williams, *Inorg. Chem.* **2007**, *46*, 965–974.
- [82] R. Wing, H. Drew, T. Takano, C. Broka, S. Tanaka, K. Itakura, R. E. Dickerson, *Nature* **1980**, *287*, 755–758.
- [83] H. Y. Zhang, A. Calzolari, R. Di Felice, *J. Phys. Chem. B* **2005**, *109*, 15345–15348.
- [84] S. S. Mallajosyula, S. K. Pati, *Phys. Rev. Lett.* **2007**, *98*, 136601.
- [85] R. A. Jishi, J. Bragin, *J. Phys. Chem. B* **2007**, *111*, 5357–5361.
- [86] J. F. Larrow, E. N. Jacobsen, Y. Gao, Y. Hong, X. Nie, C. M. Zepp, *J. Org. Chem.* **1994**, *59*, 1939–1942.
- [87] S. Katz, *Nature* **1962**, *194*, 569.
- [88] S. Katz, *Biochim. Biophys. Acta* **1963**, *68*, 240–253.
- [89] R. B. Simpson, *J. Am. Chem. Soc.* **1964**, *86*, 2059–2065.
- [90] N. Davidson, J. Widholm, U. S. Nandri, R. Jensen, B. M. Olivera, J. C. Wang, *Proc. Natl. Acad. Sci. USA* **1965**, *53*, 111–118.
- [91] L. D. Kosturko, C. Folzer, R. F. Stewart, *Biochemistry* **1974**, *13*, 3949–3952.
- [92] Z. Kuklenyik, L. G. Marzilli, *Inorg. Chem.* **1996**, *35*, 5654–5662.
- [93] A. Ono, H. Togashi, *Angew. Chem. Int. Ed.* **2004**, *43*, 4300–4302.
- [94] Y. Miyake, A. Ono, *Tetrahedron Lett.* **2005**, *46*, 2441–2443.
- [95] Y. Miyake, H. Togashi, M. Tashiro, H. Yamaguchi, S. Oda, M. Kudo, Y. Tanaka, Y. Kondo, R. Sawa, T. Fujimoto, T. Machinami, A. Ono, *J. Am. Chem. Soc.* **2006**, *128*, 2172–2173.
- [96] Y. Tanaka, S. Oda, H. Yamaguchi, Y. Kondo, C. Kojima, A. Ono, *J. Am. Chem. Soc.* **2007**, *129*, 244–245.
- [97] J.-S. Lee, M. S. Han, C. A. Mirkin, *Angew. Chem. Int. Ed.* **2007**, *46*, 4093–4096.
- [98] J. Liu, Y. Lu, *Angew. Chem. Int. Ed.* **2007**, *46*, 7587–7590.
- [99] A. A. Voityuk, *J. Phys. Chem. B* **2006**, *110*, 21010–21013.
- [100] J. Joseph, G. B. Schuster, *Org. Lett.* **2007**, *9*, 1843–1846.
- [101] J. S. Lee, L. J. P. Latimer, R. S. Reid, *Biochem. Cell Biol.* **1993**, *71*, 162–168.
- [102] P. Aich, S. L. Labiuk, L. W. Tari, L. J. T. Delbaere, W. J. Roesler, K. J. Falk, R. P. Steer, J. S. Lee, *J. Mol. Biol.* **1999**, *294*, 477–485.
- [103] A. Rikitin, P. Aich, C. Papadopoulos, Y. Kobzar, A. S. Vedenev, J. S. Lee, J. M. Xu, *Phys. Rev. Lett.* **2001**, *86*, 3670–3673.
- [104] P. Aich, R. J. S. Skinner, S. D. Wettig, R. P. Steer, J. S. Lee, *J. Biomol. Struct. Dyn.* **2002**, *20*, 93–98.
- [105] S. D. Wettig, G. A. Bare, R. J. S. Skinner, J. S. Lee, *Nano Lett.* **2003**, *3*, 617–622.
- [106] S. D. Wettig, C.-Z. Li, Y.-T. Long, H.-B. Kraatz, J. S. Lee, *Anal. Sci.* **2003**, *19*, 23–26.
- [107] S. Nokhrin, M. Baru, J. S. Lee, *Nanotechnology* **2007**, *18*, 095205.
- [108] S. S. Alexandre, J. M. Soler, L. Seijo, F. Zamora, *Phys. Rev. B* **2006**, *73*, 205112.
- [109] M. Fuentes-Cabrera, B. G. Sumpter, J. E. Šponer, J. Šponer, L. Petit, J. C. Wells, *J. Phys. Chem. B* **2007**, *111*, 870–879.
- [110] F. Moreno-Herrero, P. Herrero, F. Moreno, J. Colchero, C. Gómez-Navarro, J. Gómez-Herrero, A. M. Baró, *Nanotechnology* **2003**, *14*, 128–133.

- [111] K. Mizoguchi, S. Tanaka, T. Ogawa, N. Shiobara, H. Sakamoto, *Phys. Rev. B* **2005**, 72, 0033106.
- [112] B. Liu, A. J. Bard, C.-Z. Li, H.-B. Kraatz, *J. Phys. Chem. B* **2005**, 109, 5193–5198.
- [113] B. Q. Spring, R. M. Clegg, *J. Phys. Chem. B* **2007**, 111, 10040–10052.
- [114] S. L. Labiuk, L. T. J. Delbaere, J. S. Lee, *J. Biol. Inorg. Chem.* **2003**, 8, 715–720.
- [115] V. A. Ostrovskii, G. I. Koldobskii, N. P. Shirokova, V. S. Poplavskii, *Chem. Heterocycl. Compd. (EN)* **1981**, 412–416.
- [116] U. Ellervik, G. Magnusson, *J. Am. Chem. Soc.* **1994**, 116, 2340–2347.
- [117] C. Thibaudeau, A. Földesi, J. Chattopadhyaya, *Tetrahedron* **1998**, 54, 1867–1900.
- [118] M. J. Hynes, *J. Chem. Soc., Dalton Trans.* **1993**, 311–312.
- [119] L. Fielding, *Tetrahedron* **2000**, 56, 6151–6170.
- [120] B. Lenarcik, K. Kurdziel, M. Gabryszewski, *J. Inorg. Nucl. Chem.* **1980**, 42, 587–592.
- [121] V. I. Danilov, N. V. Zheltovsky, O. N. Slyusarchuk, V. I. Poltev, J. L. Alderfer, *J. Biomol. Struct. Dyn.* **1997**, 15, 69–80.
- [122] J. Müller, *Nature* **2006**, 444, 698.
- [123] F. Seela, T. Wenzel, *Helv. Chim. Acta* **1994**, 77, 1485–1499.
- [124] F. Seela, T. Wenzel, H. Debelak, *Nucleosides Nucleotides* **1995**, 14, 957–960.
- [125] J. Chen, N. C. Seeman, *Nature* **1991**, 350, 631–633.
- [126] P. W. K. Rothmund, *Nature* **2006**, 440, 297–302.
- [127] N. C. Seeman, *Trends Biochem. Sci.* **2005**, 30, 119–125.
- [128] D. Nykypanchuk, M. M. Maye, D. van der Lelie, O. Gang, *Nature* **2008**, 451, 549–552.
- [129] S. Y. Park, A. K. R. Lytton-Jean, B. Lee, S. Weigand, G. C. Schatz, C. A. Mirkin, *Nature* **2008**, 451, 553–556.
- [130] M.-H. Shu, C.-Y. Duan, W.-Y. Sun, Y.-J. Fu, D.-H. Zhang, Z.-P. Bai, W.-X. Tang, *J. Chem. Soc., Dalton Trans.* **1999**, 2317–2321.
- [131] S. Johannsen, S. Paulus, N. Düpre, J. Müller, R. K. O. Sigel, *J. Inorg. Biochem.* **2008**, 102, 1141–1151.
- [132] E. Ennifar, P. Walter, P. Dumas, *Nucleic Acids Res.* **2003**, 31, 2671–2682.
- [133] R. K. O. Sigel, A. Vaidya, A. M. Pyle, *Nat. Struct. Biol.* **2000**, 7, 1111–1116.
- [134] R. K. O. Sigel, A. M. Pyle, *Met. Ions Biol. Syst.* **2003**, 40, 477–512.
- [135] D. M. Gray, S.-H. Hung, K. H. Johnson, *Methods Enzymol.* **1995**, 246, 19–34.
- [136] D. M. Gray, R. L. Ratliff, M. R. Vaughan, *Methods Enzymol.* **1992**, 211, 389–406.
- [137] E. Freisinger, R. K. O. Sigel, *Coord. Chem. Rev.* **2007**, 251, 1834–1851.
- [138] I. Hirao, T. Mitsui, M. Kimoto, S. Yokoyama, *J. Am. Chem. Soc.* **2007**, 129, 15549–15555.
- [139] N. C. Seeman, *J. Theor. Biol.* **1982**, 99, 237–247.
- [140] B. Lippert, M. Leng, *Top. Biol. Inorg. Chem.* **1999**, 1, 117–142.

Received: March 25, 2008

Published Online: July 11, 2008